Food Bioscience 78 (2026) 108442

Contents lists available at ScienceDirect

Food Bioscience

journal homepage: www.elsevier.com/locate/fbio

The *in vitro* supplementation with *Sambucus nigra* extract promisingly impacts the human gut ecosystem in an individual-dependent way

Francis Aheto [a], Lena Granehäll [a], Olga Nikoloudaki [a,b,*], Martina Ben [a], Stephan Plattner [c], Marco Gobbetti [a,b], Raffaella Di Cagno [a,b], Andrea Polo [a,b]

[a] Faculty of Agricultural, Environmental and Food Sciences, Free University of Bozen-Bolzano, 39100, Bolzano, Italy
[b] International Center on Food Fermentation, 39100, Bolzano, Italy
[c] Iprona Lana SpA, 39011, Lana, Italy

ARTICLE INFO

Keywords:
European black elderberry
Plant-based bioactive compounds
Polyphenols
Gut microbiota
SHIME®

ABSTRACT

The study evaluated elderberry extract (EBE), containing 22.45% polyphenols and 10.60% total dietary fiber, on human gut ecosystems using two Simulator of the Human Intestinal Microbial Ecosystem (SHIME®) models inoculated with feces from donors with Type-B and Type-P enterotypes. EBE supplementation induced donor-specific changes, increasing acetic and propionic acids and total polyphenol content. It reshaped the gut microbiome by lowering the Firmicutes-Bacteroidetes ratio and boosting beneficial species such as *Akkermansia muciniphila*, *Bifidobacterium longum*, and *Bacteroides dorei*, while reducing harmful bacteria. Genes linked to amino acid metabolism, vitamin B6 biosynthesis, plant secondary metabolite production, and glutathione metabolism increased, with effects lasting after washout. Functional changes correlated with specific species associated with propanoate metabolism, amino acid metabolism, and plant metabolite biosynthesis. These results demonstrate that daily intake of 600 mg EBE for two weeks modulates the gut ecosystem through both individual-dependent and independent pathways, supporting personalized nutrition approaches.

1. Introduction

Diet is a key factor modulating the assembly and dynamics of gut microbiota, influencing its complex structural composition and functional properties (Polo et al., 2023; Reider et al., 2022). The challenge of modern nutrition is to valorize those diets that positively impact gut ecosystems, balancing the increased dietary complexity alongside significant nutritional insufficiencies. In fact, epidemiological studies have shown that the shift toward highly refined foods and ultra-processed beverages contributes to an increased incidence of gut dysbiosis linked to non-communicable chronic disorders such as cardiovascular diseases, obesity, and type 2 diabetes (Martinez et al., 2017; Severino et al., 2024). On the other side, diets including targeted plant-based bioactive compounds can exert a significant role in addressing the gut ecosystems toward a more balanced status (Wang et al., 2024). As a mainstay of the diet, the World Health Organization (WHO) recommends a minimum daily intake of 400 g of fruits and vegetables (about 5 portions) per person to have enough intake of key bioactive compounds. However, global consumption remains alarmingly lower despite the well-established health benefits. In Europe, only ca. 33% of adults meet this recommendation, with significant variation between countries, while this percentage decreases to 12.3% in America (CDC, 2022; Eurostat, 2022). Consequently, there is a growing need for dietary interventions, including functional and nutraceutical supplementation, to increase the intake of plant-based bioactive compounds, aiming to promote healthier conditions in gut ecosystems.

Polyphenols and dietary fibers from fruits and vegetables have emerged as promising candidates (Manning & Gibson, 2004; Pandey et al., 2015). Recently, European black elderberry (*Sambucus nigra L.*) fruit has been revalued as functional food or proposed as an ingredient for functional foods due to its high polyphenols content, including anthocyanins, flavanols, and phenolic acids with proven antioxidant, anti-inflammatory, anticarcinogenic, and immunomodulatory effects (Młynarczyk et al., 2018; Reider et al., 2022). This interest goes beyond its conventional use as a juice or colorant, shifting towards the extraction and standardization of polyphenols like anthocyanins for the development of targeted dietary supplements and nutraceuticals, as most polyphenols are unstable during processing or are lost during

* Corresponding author. Faculty of Agricultural, Environmental and Food Sciences, Free University of Bozen-Bolzano, 39100, Bolzano, Italy.
E-mail address: olga.nikoloudaki@unibz.it (O. Nikoloudaki).

https://doi.org/10.1016/j.fbio.2026.108442
Received 23 September 2025; Received in revised form 5 February 2026; Accepted 6 February 2026
Available online 10 February 2026

juicing (Xiao, 2022).

While polyphenols have low absorption in the upper gastrointestinal tract, the extensive transformation into phenolic metabolites by colon microbiota suggests potential prebiotic effects (Bresciani et al., 2020; Vinelli et al., 2022). Recently, a "duplibiotic" action has been proposed for polyphenols: on one side, they may reshape the composition of the intestinal microbiota by exhibiting antimicrobial properties against specific pathobionts; on the other side, they may have a prebiotic effect through their metabolization by the microbiota (Rodríguez-Daza et al., 2021).

Some studies suggested that polyphenols and dietary fibers work synergistically as co-substrates to promote the growth of beneficial bacteria such as *Bifidobacteria* spp. and *Bacteroides* spp., potentially reducing the Firmicutes-Bacteroidetes ratio, and yielding beneficial metabolites like short-chain fatty acids (SCFAs) associated with positive physiological outcomes (Graf et al., 2015; Tuohy et al., 2003).

However, the metabolism of polyphenols is highly complex and strictly linked to the individual gut microbiome composition, resulting in different enzymatic and metabolic pathways, which may allow for classification into specific enterotypes, metabotypes or nutritional phenotypes (Stevens and Maier, 2016). Consequently, polyphenols do not have a univocal impact on the gut microbiome, while their impact on commensal microbiota modulation and metabolism significantly varies depending on their molecular structure, dosage, and the structure of microbial populations (Plamada and Vodnar, 2021). Despite the growing body of research dealing with the effects of polyphenol extracts or polyphenol-rich foods on the human gut microbiome, more targeted investigations are needed to distinguish common effects and individual-dependent impacts across different polyphenols. However, the inherent complexity of the human gut ecosystem makes comprehensive clinical trials challenging and cost-intensive. Most gut-polyphenols interrelationship studies have relied on animal models, especially mice, whose findings may not be fully translational for human physiological responses (Beresford-Jones et al., 2022). Nevertheless, most studies through human gut models have been constrained by experimental designs using a single fecal inoculum, failing to consider the role of inter-individual human gut microbiome variability (Bäckhed et al., 2012).

To address these gaps, we employed a novel experimental approach to investigate the effect of a new polyphenol-standardised European black elderberry extract on two different gut ecosystems that are representative of a bigger cohort of people adhering to the Mediterranean diet by feeding the Simulator of the Human Intestinal Microbial Ecosystem (SHIME®), the validated multicompartmental model system reproducing a stable human gut microbiota from fecal samples (Van Den Abbeele et al., 2010). Since such an approach allows to exclude a priori any interference between other dietary factors and human physiology overlaps, as well invasive sampling (Yang et al., 2022), we believe it represents the most suitable technology to obtain preliminary microbiome-level *in vitro* insights concerning the gut ecosystem-specific impact (Li et al., 2020; Molly et al., 1993). In addition, although previous studies investigating the impact of European black elderberry fruit juice (Teets et al., 2024) or extract (Reider et al., 2022) highlighted potential beneficial effects on gut microbiota, they primarily relied on 16S rRNA sequencing, with no functional insights, and they did not assess the impact on SCFAs synthesis, leaving significant gaps in our understanding. In this study, shotgun metagenomics, SCFAs, and total polyphenols content (TPC) analyses on lumen samples from the SHIME® simulation were carried out to assess the evolution of colon tract ecosystems in response to the extract supplementation. First, such a holistic approach has been adopted to study the role played by polyphenol-standardised European black elderberry extract on gut ecosystems.

2. Materials and methods

2.1. Raw materials

The European black elderberry extract (EBE, also known as Elder-Craft® 14%) was provided by Iprona Lana SpA (Lana, Italy). Table 1 reports the major nutritional and bioactive composition of EBE. The extract is standardized to a defined amount of polyphenols (22.45%) and contains total dietary fiber (10.60%; soluble and insoluble). The predominant polyphenolic component is anthocyanins (67.7% of total polyphenols), which include cyanidin 3-sambubioside-5-glucoside, cyanidin 3,5-diglucoside, cyanidin 3-sambubioside, and cyanidin 3-glucoside. The other polyphenols include flavonoids (10.42% of total polyphenols), such as rutin and isoquercitrin, and minor amounts of phenolic acids like chlorogenic acids.

2.2. SHIME® configuration and experimental design

The SHIME® (ProDigest, Gent, Belgium) configuration comprised two identical units operating in parallel (S1 and S2). Each unit consisted of three double-jacketed bioreactors maintained at a temperature of 37 °C, simulating the stomach and small intestine (ST/SI), proximal colon (PC), and distal colon (DC), respectively (Polo et al., 2023). The PC and DC bioreactors were filled with 500 and 800 mL, respectively, of adult L-SHIME® growth medium (ProDigest, Gent, Belgium). The pH was set between 5.75 and 5.9, and between 6.6 and 6.9 in PC and DC, respectively, and was computer-controlled using 0.5 mol/L HCl and 0.5 mol/L NaOH. The ST/SI bioreactors were set at pH 2. The feces of two different representative healthy donors were used to inoculate PC and DC bioreactors of S1 and S2, respectively. Fecal donors were selected from a cohort of 40 individuals (ages 19–50) adhering to a Mediterranean diet, as described by Da Ros et al. (2021). Volunteers were without chronic intestinal or metabolic disorders, non-smokers, not pregnant, and had no history of drug, antibiotic, probiotic or prebiotic use in the past 6 months. Their Mediterranean Diet Score (MDS), calculated according to Gutiérrez-Díaz et al. (2016), ranged from 5 to 8, indicating good adherence to the diet. Aiming to choose representative fecal inocula, fecal samples of volunteers were collected in sterile bags, immediately mixed with RNA later solution, and homogenized. Microbiota composition and SCFAs content were analyzed. Donor selection was based on clustering fecal microbiota data and SCFAs profiles using the Manhattan distance matrix and Ward D2 method. Partial

Table 1
Main composition of the European black elderberry (EBE) extract (w/w, dry basis), and daily dose of each component supplied during the SHIME simulation. * 600 mg was the daily dose of European black elderberry extract.

Class of compounds	Composition of the extract (mg/kg)	Daily dose supplied during the SHIME® simulation (mg/600 mg*)
Total polyphenols	224500	134.7
Anthocyanin (as cya-3-glu)	152000	91.2
Flavonoids	23397	14.0
Total dietary fiber	106000	63.6
Carbohydrates	75000	45.0
Proteins	7200	4.3
Fat	200	0.1
Ash	3000	1.8

least-squares discriminant analysis (PLS-DA) was performed to model the relationship between diet adherence and microbiota (Da Ros et al., 2021). The procedure was approved by the Ethics Committee of the Free University of Bozen on July 17, 2019, with informed consent obtained from all participants. The fecal inocula were prepared as described by Molly et al. (1993) and inoculated at 5% (v/v) within 1 h after collection. The SHIME® cabinet and its accompanying software were operated in accordance with the manufacturer's instructions (ProDigest, Ghent, Belgium). The simulation run consisted of a 14-day stabilization period to allow microbiota adaptation, followed by a 14-day basal period (control period). During stabilization and control periods, 140 mL of adult L-SHIME® growth medium (ProDigest, Gent, Belgium) and 60 mL of pancreatic juice (12.5 g/L $NaHCO_3$, 0.9 g/L pancreatin and 6 g/L oxgall) were added to ST/SI bioreactors 3 times/day (to simulate 3 daily meals), and then transferred to the colon bioreactors. Feeding cycles occurred on a fixed schedule, allowing for an 8-h fermentation period between each cycle. During the control period, lumen samples were collected from PC and DC bioreactors 3 times/week, 10 min before the start of the next feeding cycle. The concentration of SCFAs (acetate, propionate, and butyrate) was measured to monitor the fermentative activity of the microbial communities and to assess the reproducibility and stability of gut ecosystems. The steady-state control period was followed by a 2-week treatment period during which a daily dosage of 600 mg/day of the EBE (Table 1) was supplemented to the basal feed (adult L-SHIME® growth medium). This dosage is coherent with the polyphenols amount deriving from the WHO recommendation of daily fruit and vegetables consumption (Reider et al., 2022). Finally, a 1-week washout period without EBE supplementation was implemented. During the simulation, all bioreactors were continuously stirred, flushed once daily with sterile N_2, and monitored for constant volume and pH stability. Samples of lumen (50 mL) were collected from both PC and DC bioreactors at the end of the control period (T0), after one (T1) and two (T2) weeks of the treatment period, and at the end of the washout period (T3) to investigate the ecosystems at baseline, short- and mid-term, and post-intervention points, respectively, in agreement with established protocols (Polo et al., 2023; Van den Abbeele et al., 2010). They were stored at −20 °C for a maximum of 3 weeks and then subjected to SCFAs, TPC and shotgun metagenomics analyses.

2.3. SCFAs and TPC quantification

The concentrations of acetic, propionic, and butyric acids in lumen and fecal samples were analyzed since they are the main SCFAs (>95%) resulting from the metabolic fermentation of gut microbiota (Nabizadeh et al., 2023). Luminal samples from the SHIME® bioreactors were centrifuged at 9400×*g* for 10 min at 4 °C, and the supernatants were filtered through a 0.2 μm filter (Whatman, Darmstadt, Germany). One hundred microliters of each filtrate was mixed with 400 μL of 5 mmol/L sulfuric acid (eluent). The mixtures were filtered and transferred into autosampler vials for the analysis. The fecal samples from volunteers were prepared as described by (Da Ros et al., 2021). The concentrations in both luminal and fecal samples were determined by High-Performance Liquid Chromatography (HPLC) analysis. The HPLC system (UltiMate 3000 series, Thermo Fisher Scientific, Waltham, MA, USA) was equipped with an Aminex HPX-87H column (ion exclusion, Bio-Rad), a UV detector operating at 210 nm, and a PerkinElmer 200a refractive index detector (Tlais et al., 2021). Elution was at 70 °C, with a flow rate of 0.6 mL min^{-1}, using 5 mmol/L sulfuric acid as the mobile phase (isocratic). The SCFAs standards were purchased from Sigma-Aldrich (Steinheim, Germany). The peak areas were integrated, and the absolute concentrations (mmol/L) were calculated based on the calibration curve equation of each SCFA.

The TPC of each luminal sample was quantified using methanol/water-soluble extracts (MWSE), following the extraction method described by Tlais et al. (2021) adapted as follow. A 1 mL aliquot of luminal samples was mixed with 1 mL of methanol/water solution (80:20, v:v). The mixture was sonicated at 35 kHz frequency for 60 min using a Sonorex™ ultrasonic bath (Bandelin, Berlin, Germany). After sonication, the mixtures were centrifuged at 9400×*g* for 10 min at 4 °C, and the resulting supernatants were filtered (0.2 μm). The TPC was determined using the Folin-Ciocalteu method (Singleton & Rossi, 1965). For TPC quantification, 20 μL of each MWSE extract was diluted with 1.58 mL of distilled water, mixed with 100 μL of Folin-Ciocalteu reagent, and incubated for 8 min at room temperature (22 ± 1 °C). Then, 300 μL of sodium carbonate (20%, w/v) was added, and the samples were incubated at 40 °C for 30 min. Absorbance was measured at 740 nm. The TPC was expressed as gallic acid equivalents (GAE mg/L). Both SCFAs and TPC analyses were performed in triplicate.

2.4. Shotgun metagenomics analysis

To comprehensively characterize the structure and potential functionality of gut microbiome within the model ecosystems and to assess the potential impact of the elderberry extract, total genomic DNA was extracted from the SHIME® luminal samples (1 mL) using the DNeasy® PowerSoil® Pro Kit (Qiagen, Hilden, Germany) according to the manufacturer's instructions. Three replicate DNA extractions were performed for each sample, and all downstream analyses were conducted in triplicate. The yield and purity of each DNA extract were confirmed using a NanoDrop™ One/OneC Microvolume UV-Vis Spectrophotometer (Thermo Fisher Scientific, Waltham, MA, USA). Sequencing libraries were prepared using the Illumina DNA Prep (M) Tagmentation kit (Illumina, #20060059), and purified via a double-sided bead purification method following the Illumina protocol. Library concentrations were quantified with the Quant-iT™ 1X dsDNA Assay Kit, HS (Life Technologies, #Q33232) using the Varioskan LUX Microplate Reader (Thermo Fisher Scientific, #VL0000D0). The base pair length (bp) was assessed with the D5000 ScreenTape Assay (Agilent, #5067-5588/9) on the TapeStation 4150 (Agilent, #G2992AA). The pooled libraries were then quantified with the Qubit 1x dsDNA HS kit (Life Technologies, #Q33231) using the Qubit® 3.0 Fluorometer (Life Technologies, #Q33216), and their base pair length was reassessed. Finally, the pooled libraries were sequenced on the Novaseq XPlus platform (Illumina) at an average depth of 20 GB per sample. Sequencing quality control was performed using FastQC. Adapter trimming and removal of low-quality bases (Phred score < Q30) were conducted using fastp (Chen et al., 2018), followed by removal of duplicate reads with SeqKit (Shen et al., 2024). Across samples, >90% of reads passed Q30 filtering, yielding an average of 70,986,844 reads per sample (range: 46-117 million).

After quality filtering and deduplication of the sequence data, species-level taxonomic classification was performed using MetaPhlAn 4 (Blanco-Míguez et al., 2023) with the mpa_vJan21_CHOCOPhlAnSGB_202103 database. The phyloseq package in R Studio was utilized for downstream analysis of bacterial communities. To establish the functional potential of the bacterial community and its impact on the gut, functional profiling was performed using HUMAnN 3 v3.6 (Beghini et al., 2021) with default options and the UniProt/Uniref 201901b database. Gene family abundance tables were converted to Kyoto Encyclopedia of Genes and Genomes database (KEGG) orthologies (KO) and normalized to copies per million (CPM).

2.5. Statistical analyses

For SCFAs and TPC concentrations, one-way ANOVA followed by post hoc Tukey's tests was employed to identify statistically significant differences among sampling points within each single bioreactor. At each simulation phase, differences between the two SHIME® units were evaluated using a two-sided unpaired Student's t-test. Significance was determined at p-values (P) < 0.05. Alpha diversity of microbiome in different colon tracts and at the different time points for each SHIME® unit was assessed using the Shannon index and Kruskal-Wallis test to measure species richness and evenness within each sample. Bray-Curtis

dissimilarity metrics were employed for Beta diversity analysis, visualized through principal coordinate analysis (PCoA) to compare microbial community composition between samples. Microbiome Multivariable Association with Linear Models (MaAsLin2) was applied to analyze the differential abundance of microbial taxa across the experimental timeline in different colon tracts and donors. MaAsLin2 was also used to analyze the differential abundance of potential pathways and functional genes across the simulation phases in different colon tracts and donors. Nonmetric Multidimensional Scaling (NMDS) ordination was conducted utilizing the 'cmdscale' and 'metaMDS' functions from the 'base' R package, to discriminate between the functional profiles derived from HUMAnN analysis, calculated using Jaccard's distance metric. PERMANOVA (Adonis2) was used to assess the marginal effects of the colon: SHIME unit®: simulation phase interaction on microbiota and functional profiles, with significance determined at $P < 0.05$ and the proportion of variance explained (R^2) reported. Spearman correlation analyses were conducted between bacterial species and metabolic pathways that exhibited significant temporal changes within each colon tract. False discovery rate (FDR) correction was applied to adjust for multiple comparisons. All statistical analyses were performed using R Studio.

3. Results

3.1. Donors selection

The clustering analysis grouped the individuals into two main clusters (Supplementary Fig. 1, Da Ros et al. (2021)). PLS-DA validated the statistical significance of clustering, with components 1 and 2 explaining 77.9% and 0.1% of the total variance, respectively. Therefore, to inoculate the SHIME® bioreactors, we randomly selected one fecal donor as representative of each distinct microbiota and SCFAs cluster.

3.2. Elderberry extract affects SCFAs production and polyphenol metabolism in an ecosystem-specific manner

Overall, before and after one and two weeks of elderberry extract supplementation, the SCFAs showed distinctive profiles in different SHIME® units (S1 and S2) for both colon tracts, with the only exception of acetic acid in DC at T1 and T2 (Table 2). S1 had relatively higher levels of butyric acid, while S2 had relatively higher levels of acetic (in PC) and propionic acids (in both colon tracts). Compared to T0, the EBE intake increased ($P < 0.05$) acetic acid concentration only in DC of S1 at T1 and in DC of S2 at T2, while, during the washout period (T3), an overall decrease was observed, except for the PC of S2. Propionic acid had a significant increase during the intake of EBE only in S1, both in PC (at both T1 and T2) and DC (at T2). Except for DC of S2, the propionic acid concentration decreased at T3 compared to T0, in both SHIME® units and colon tracts. The levels of butyric acid did not vary significantly during the simulation, except for a decrease observed at T3 in the DC of S2.

Across both colon tracts, S1 and S2 displayed different TPC levels at each time point, except at T3 in the DC, where no significant difference was observed. TPC levels were significantly higher in S1 than S2 (except in DC at T1 and T3). TPC generally increased ($P < 0.05$) during the intake of EBE in both colon tracts and both SHIME® units, and, after the intake interruption (T3), the concentrations remained significantly higher than T0. With the only exception of S1 in PC, TPC levels further increased at T3 compared to the treatment period.

3.3. Elderberry extract supplementation differentially affected the gut taxonomic composition

The relative abundance plot of the top 15 genera (Supplementary Fig. 2A) and the top 20 species (Supplementary Fig. 2B) revealed differences in bacterial community composition between the colon tracts of two SHIME® units. Overall, the bacterial microbiota of S1 was dominated by *Bifidobacterium*, *Phocaeicola*, and *Bacteroides*, while S2 was dominated by *Prevotella* and *Megamonas*. Both DCs had a high relative abundance of *Akkermansia*. Overall, the DCs showed higher species diversity (177 species) compared to the PCs (58 species). At T0, the most abundant species in the PC of S1 included *Bifidobacterium longum* (36.07%), *Phocaeicola dorei* (15.57%), and *Bacteroides ovatus* (7.21%), while *Akkermansia muciniphila* (13.37%), *Bacteroides uniformis* (11.31%), and *B. longum* (11.17%) were dominant in DC. For S2, the most abundant species at T0 were *Megamonas funiformis* (43.69%), and *Prevotella copri* Clade A (25.16%) in PC, and *A. muciniphila* (11.58%), *B. uniformis* (10.39%) and *P. dorei* (10.33%) in DC. The Firmicutes-Bacteroidetes (F/B) ratio was significantly modulated by EBE intake (Supplementary Fig. 2C). In PC of S2 and DC of S1, it showed a continuous decline during the simulation phases. In PC of S1 and DC of S2, although it had a different evolution, it reached final values that are

Table 2
Short-chain fatty acids (SCFAs) concentrations (mmol/L) and total polyphenol content (TPC) expressed as gallic acid equivalent (mg/l GAE), measured in the proximal (PC) and distal colon (DC) of both SHIME® units (S1 and S2) across baseline (T0), one and two weeks of elderberry extract intake (T1 and T2, respectively), and following a one-week washout (T3). Data represents the mean ± standard deviation from three independent analyses. For each compound, values in the same row with different superscript letters indicate statistically significant temporal differences within each colon tract, as determined by one-way ANOVA followed by Tukey–Kramer post hoc comparisons ($P < 0.05$). At each time point and for each colon tract, an asterisk in the same column indicates a statistically significant difference between the two SHIME® units (S1 and S2), based on a two-sided unpaired Student's t-test ($P < 0.05$).

Compound	Colon tract	SHIME® unit	Concentration			
			T0	T1	T2	T3
Acetic acid (mmol/L)	**PC**	**S1**	$23.43 \pm 0.43^{a*}$	$23.77 \pm 0.68^{a*}$	$22.52 \pm 0.22^{a*}$	$9.77 \pm 2.07^{b*}$
		S2	$29.01 \pm 1.18^{ab*}$	$29.41 \pm 0.55^{ab*}$	$30.32 \pm 0.78^{a*}$	$27.69 \pm 0.85^{b*}$
	DC	**S1**	$41.78 \pm 0.46^{b*}$	44.98 ± 1.44^{a}	44.34 ± 0.42^{ab}	$31.46 \pm 1.19^{c*}$
		S2	$40.79 \pm 0.33^{b*}$	42.38 ± 1.10^{ab}	43.57 ± 0.59^{a}	$37.63 \pm 1.02^{c*}$
Propionic acid (mmol/L)	**PC**	**S1**	$7.06 \pm 0.15^{b*}$	$9.82 \pm 0.36^{a*}$	$11.58 \pm 0.69^{a*}$	$4.85 \pm 1.36^{c*}$
		S2	$25.21 \pm 0.31^{a*}$	$27.74 \pm 1.18^{a*}$	$27.26 \pm 1.89^{a*}$	$19.80 \pm 0.56^{b*}$
	DC	**S1**	$16.32 \pm 0.24^{b*}$	$17.35 \pm 0.64^{b*}$	$21.15 \pm 0.40^{a*}$	$13.29 \pm 1.23^{c*}$
		S2	$35.24 \pm 0.27^{a*}$	$36.84 \pm 0.31^{a*}$	$36.65 \pm 0.50^{a*}$	$29.87 \pm 2.15^{a*}$
Butyric acid (mmol/L)	**PC**	**S1**	$10.62 \pm 0.68^{a*}$	$9.90 \pm 0.06^{a*}$	$7.54 \pm 0.16^{a*}$	$8.48 \pm 0.73^{a*}$
		S2	$0.94 \pm 0.05^{a*}$	$0.90 \pm 0.05^{a*}$	$0.65 \pm 0.02^{a*}$	$0.73 \pm 0.08^{a*}$
	DC	**S1**	$12.94 \pm 0.10^{a*}$	$12.82 \pm 0.34^{a*}$	$11.05 \pm 0.31^{a*}$	$12.99 \pm 1.44^{a*}$
		S2	$4.60 \pm 0.11^{a*}$	$4.29 \pm 0.23^{a*}$	$4.35 \pm 0.05^{a*}$	$2.92 \pm 0.26^{b*}$
TPC (mg/L GAE)	**PC**	**S1**	$107.00 \pm 0.35^{d*}$	$471.25 \pm 7.75^{c*}$	$585.50 \pm 10.00^{a*}$	$548.12 \pm 5.88^{b*}$
		S2	$94.00 \pm 3.00^{d*}$	$436.63 \pm 7.38^{c*}$	$513.50 \pm 8.75^{b*}$	$572.25 \pm 10.50^{a*}$
	DC	**S1**	$119.63 \pm 1.87^{d*}$	$481.75 \pm 14.00^{b*}$	$378.12 \pm 0.53^{c*}$	600.63 ± 6.63^{a}
		S2	$77.75 \pm 0.71^{d*}$	$521.87 \pm 8.13^{b*}$	$300.13 \pm 13.88^{c*}$	615.25 ± 7.00^{a}

lower than those of the baseline (T0), even after the washout period. Overall, S2 had higher F/B ratios in the PC, while S1 had higher F/B ratios in DC.

Alpha diversity showed significant changes during the treatment period in all colon tracts and both SHIME® units, except the DC of S1 (Fig. 1A). In the PC of S1, changes were all over the time points, while for S2, significant changes were observed from T0 to T2 in the PC, and from T1 to T3 in the DC. Beta diversity (Fig. 1B) highlighted that the different donor (i.e. the SHIME® unit) was the primary driver of microbial community composition, explaining a significant proportion of variance (~79% in DC, ~81% in PC, $P = 0.001$), while time (i.e. the simulation phases) had a smaller but still significant effect (~10.5% in DC, ~8.7% in PC, $P = 0.001$), with S1 showing stronger temporal effects ($R^2 = 0.945$ in DC, $R^2 = 0.975$ in PC) compared to S2 ($R^2 = 0.618$, $P = 0.011$).

The differential abundance analysis revealed species with significant changes in relative abundance during EBE intake and washout compared to baseline (Supplementary Fig. 3). Indeed, the EBE intake induced a significant temporal shift in the PCs in thirteen out of 58 species (22.41%), while 127 out of 177 species (71.75%) shifted significantly in the DCs of one or both SHIME® units. Comparative analysis of the species with differential abundance (Fig. 2) highlighted the taxa evolving with a common trend in both SHIME® units across the simulation phases. They were 4 and 15 species in PCs and DCs, respectively. In the PCs, *Leifsonia* sp. C5G2 and *Phytobacter diazotrophicus* expanded only in the short-term period during the intake of EBE (T1), while *E. durans* and *Pseudomonas putida* expanded only after the intake interruption. In DCs, *Achromobacter xylosoxidans*, *Acinetobacter ursingii*, *Leifsonia* sp. C5G2 and *P. diazotrophicus* increased after the intake of EBE only in the short-term period (T1), *Alistipes finegoldii* and *Alistipes onderdonkii* reached the highest abundance at the longer term intake (T2), *Parabacteroides distasonis* and *Citrobacter freundii* expanded with the intake only at the short-term period, and after the intake interruption, *C. scindens* and *Enterococcus faecalis* decreased during the intake, *E. durans* expanded only after the intake interruption (T3), while *Exiguobacterium chiriqhucha*, *Klebsiella michiganensis*, *Klebsiella oxytoca* and *Raoultella ornithinolytica* decreased due to the EBE intake but increased during the washout period (T3).

3.4. Elderberry extract supplementation influenced differential functional potential of gut metagenomes

Besides the taxonomic variations, the gut microbiome metabolic potential significantly changed at the end of treatment. Several significantly differentially abundant pathways (12 main pathways) were observed. The most abundant pathways included amino acid metabolism, biosynthesis of other secondary metabolites, carbohydrate metabolism, energy metabolism, metabolism of cofactors and vitamins, and metabolism of terpenoids and polyketides. S1 had a higher abundance of these processes in both colon tracts compared to S2 (Fig. 3). The Non-metric Multidimensional Scaling (NMDS) plot highlighted that the SHIME® unit (S1 or S2) and the colon tract (PC and DC) were the primary factors driving the clustering of functional genes, with simulation phases (i.e., before, during, and after the intake of EBE) having a lesser effect (Fig. 4). This is supported by the significant colon tract: SHIME® unit: simulation phase interaction ($P = 0.001$, $R^2 = 0.04016$), as revealed by PERMANOVA (Adonis2). Pairwise comparisons confirmed significant differences between S1 and S2 ($R^2 = 0.37921$, $P = 0.001$), and between PC and DC ($R^2 = 0.2081$, $P = 0.001$). S1 exhibited stronger temporal effects in the PC ($R^2 = 0.95901$, $P = 0.001$), while S2 showed stronger temporal effects in the DC ($R^2 = 0.92784$, $P = 0.002$). The evaluation of top functional features using MaasLin2 revealed ecosystem-specific significant changes in functional genes abundance during the treatment and washout phases compared to baseline, which are overall described in Supplementary Fig. 4. Comparative analysis of differentially abundant functional pathway-associated genes revealed shared temporal trends in both SHIME® units, with genes related to 6 pathways in the PC and 8 in the DC showing consistent changes over time (Fig. 5). In PCs, genes associated with fructose and mannose metabolism, glycine, serine and threonine metabolism, and streptomycin biosynthesis increased in the short-term period during the intake of EBE (T1) and after the intake interruption (T3). Vitamin B6 biosynthesis genes increased consistently during the EBE intake period (T2 and T3), while those related to the biosynthesis of plant secondary metabolites peaked at longer-term intake (T2). Genes linked to *Escherichia coli* biofilm formation decreased at T1 and T2 but increased at T3. In DCs,

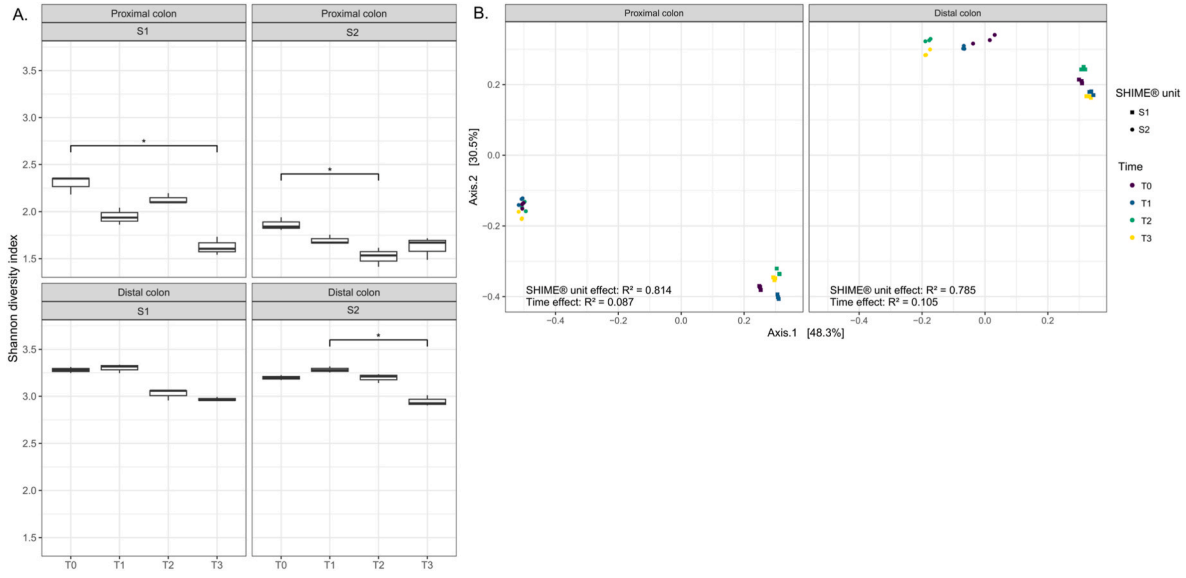

Fig. 1. (A) Alpha diversity of bacterial communities composition based on Shannon diversity index during the simulation phases for both proximal and distal colon tracts and both SHIME® units (S1 and S2). T0, T1, T2, and T3 mean before the intake of elderberry extract, after one and two weeks of intake, and after the washout period, respectively. The asterisk represents significant changes ($P < 0.05$). **(B)** Principal coordinate analysis (PCoA) of bacterial community composition based on Bray-Curtis dissimilarity metrics during the experimental phases (T0, T1, T2, T3) for both proximal and distal colon tracts of both SHIME® units (S1 and S2). Permutation-based Adonis2 test assessed the effects of the SHIME® unit, simulation phase (time), and their interaction. Significant effects due to SHIME® unit, simulation phase, and SHIME® unit × simulation phase interaction were observed (all with $P < 0.05$). Betadisper test confirmed consistent dispersions, and Tukey's HSD test showed minimal significant differences between time points.

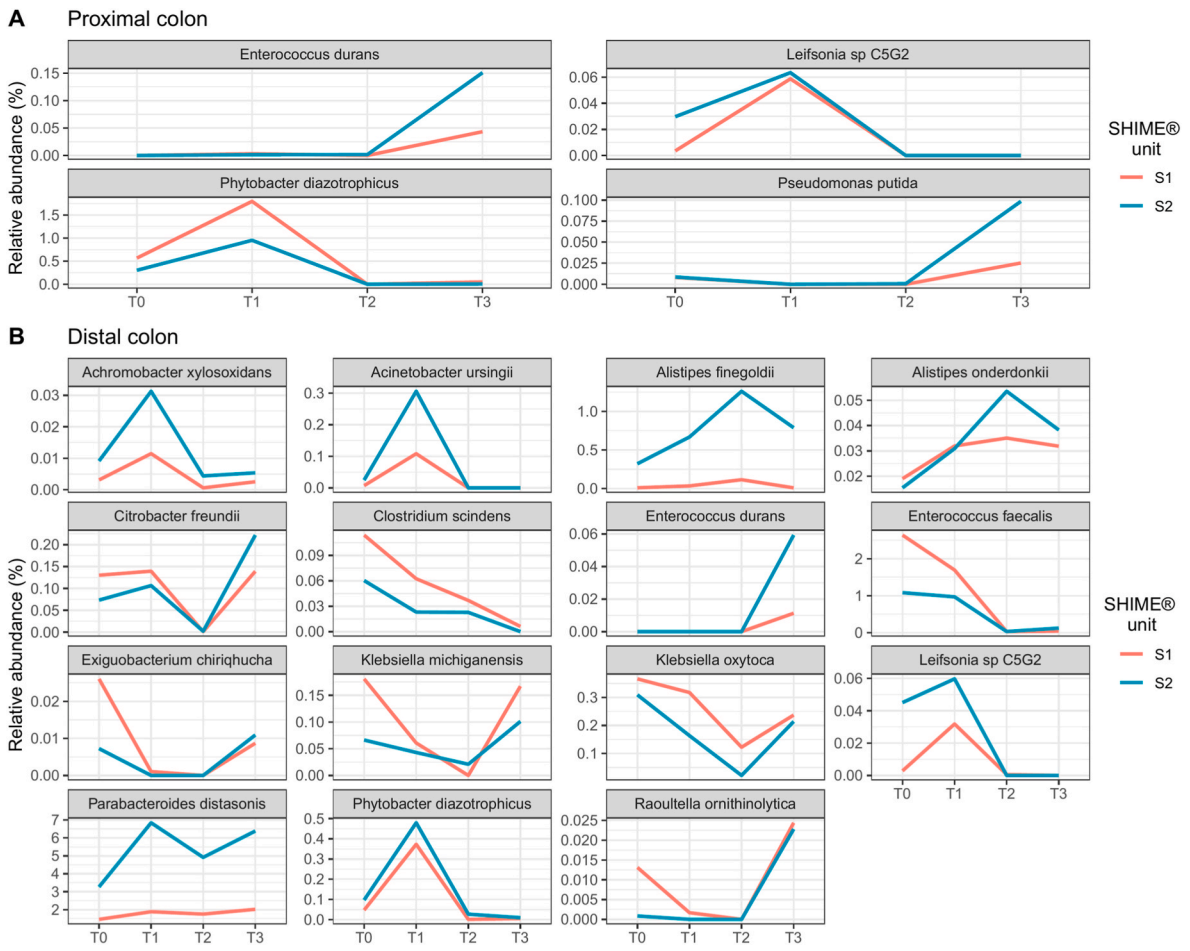

Fig. 2. Common trends in the modulation of species abundance across both SHIME® units (S1 and S2) in **(A)** the proximal colon (PCs) and **(B)** the distal colon tracts (DCs), at baseline (T0), after one (T1) and two (T2) weeks of elderberry extract intake, and after one week of washout (T3). Species were included in the comparative analysis if they exhibited significant temporal changes in the PC or DC of at least one SHIME® unit, as determined by differential abundance analysis using MaAsLin2 with false discovery rate correction ($q < 0.05$; see Supplementary Fig. 3).

genes involved in alanine, aspartate and glutamate metabolism, teichoic acid biosynthesis, phenylpropanoid biosynthesis, N-glycan biosynthesis, and valine, leucine, and isoleucine degradation increased at T1 and T3. Genes involved in glutathione metabolism and propanoate metabolism increased at T1 and T2 but decreased at T3. Conversely, genes related to carbapenem biosynthesis decreased at T1 and T2 but increased at T3. Overall, S1 exhibited a higher abundance of these functional pathways than S2 in both colon tracts. The Spearman correlations revealed significant species driving pathway-associated genes in S1 and S2 colon tracts (*padj* < 0.05, <0.01, or < 0.001), excluding the PC of S2, which showed no significant differential species abundance (Fig. 6). The correlations were cross-validated with the differential abundance profiles of both species and pathway genes (Supplementary Figs. 3 and 4) to identify co-occurring patterns, thereby strengthening potential causal relationships. This integrative approach emphasized only those species–pathway gene relationships that exhibited both strong correlations (padj <0.01 or < 0.001) and concurrent significant abundance changes. In the PC of S1, *P. diazotrophicus* exhibited a positive correlation with glycine, serine, and threonine metabolism genes, with increased abundance at both T1 and T3. Meanwhile, *P. dorei* was positively associated with genes related to sphingolipid metabolism, neuroactive ligand-receptor interaction, and streptomycin biosynthesis, showing increased abundance at T1. A group of species, including *P. distasonis*, *Collinsella aerofaciens*, *Clostridium butyricum*, *B. ovatus*, and *Aeromonas caviae*, showed positive correlations with drug metabolism pathway, with increased abundance observed at T2. Additionally, *C. butyricum*, *B. ovatus*, *P. distasonis*, and *B. longum* exhibited increased abundance at T2, positively correlating with genes associated with the biosynthesis of various plant secondary metabolites. In the DC of S1, glycolysis/gluconeogenesis was positively correlated with *Bacteroides eggerthii*, showing increased abundance at T2 and T3. Alanine, aspartate, and glutamate metabolism was positively correlated with *B. eggerthii*, with increased abundance at T1 and T3. Glutathione metabolism positively correlated with *E. coli*, *C. freundii*, *K. oxytoca*, *Bacteroides salyersiae*, and *P. diazotrophicus*, with increased abundance at T2. Amino sugar and nucleotide sugar metabolism correlated with *B. eggerthii*, *Megasphaera micronuciformis*, and *Alistipes putredinis*, showing increased abundance at T2 and T3. Inositol phosphate metabolism positively correlated with *B. ovatus*, with increased abundance at T2. Citrate cycle was positively correlated with *Enterococcus faecium*, *K. oxytoca*, and *Enterococcus gallinarum*, with increased abundance at T1 and T2. Propanoate metabolism positively correlated with *E. coli*, *C. freundii*, *K. oxytoca*, *Enterococcus malodoratus*, *E. gallinarum*, and *E. faecium*, with increased abundance at T1. In the DC of S2, the abundance of genes involved in valine, leucine, and isoleucine degradation showed an increase at T1, positively correlating with *A. xylosoxidans*. At T2, carbapenem biosynthesis decreased, positively correlating with *Klebsiella aerogenes* and negatively correlating with *A. muciniphila*. Selenocompound metabolism was elevated at T2, with positive correlations to *Bacteroides clarus*, *A. putredinis*, *Clostridium innocuum*, *Clostridium* sp. AM33_3, and *E. faecalis*. Finally, glutathione metabolism increased at both T1 and T2, exhibiting a positive correlation with *A. xylosoxidans*.

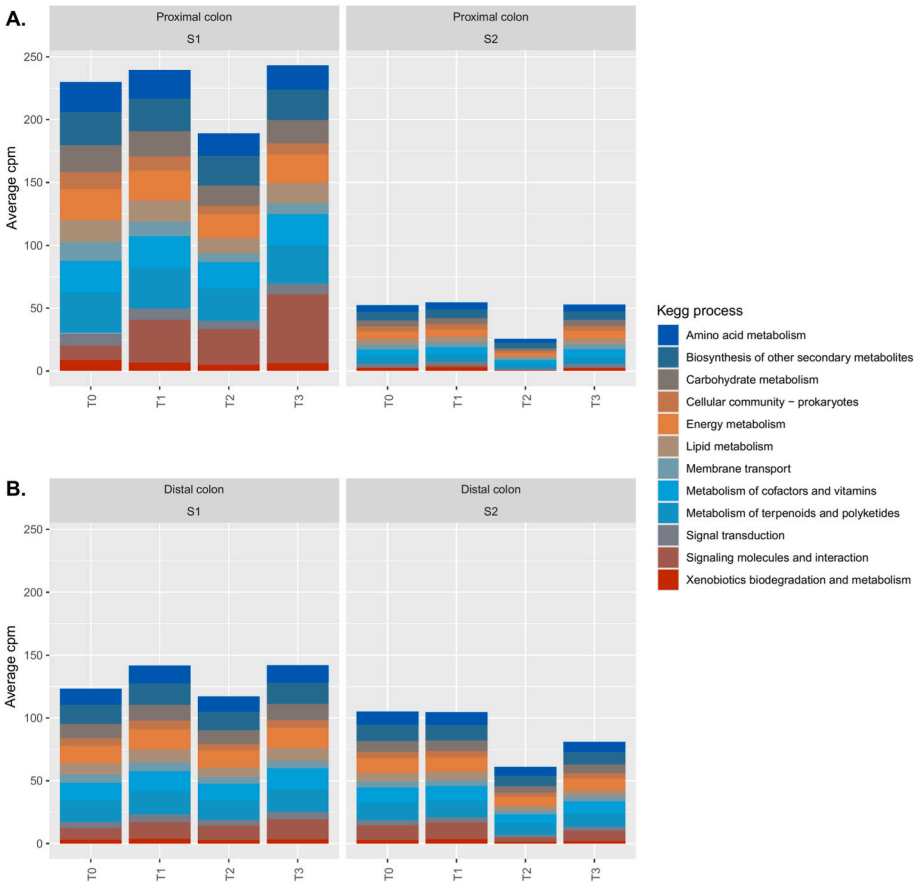

Fig. 3. Absolute abundance (mean counts per million, cpm) of KEGG pathways in **(A)** the proximal colon (PC) and **(B)** the distal colon (DC) tracts of both SHIME® units (S1 and S2) across experimental phases: baseline (T0), after one (T1) and two (T2) weeks of elderberry extract intake, and after one week of washout (T3).

4. Discussion

Advancements in personalized nutrition have identified the interindividual gut microbiome variability as a key factor addressing the metabolism and health benefits of plant bioactive compounds like polyphenols (Kerimi et al., 2020). This variability influences distinct metabolic responses due to individual-specific shifts in commensal microbiota composition and functionality (De Paepe et al., 2020). Through an *in vitro* simulation employing two SHIME® units stabilized with fecal microbiota from two individuals that are representative of a bigger cohort of people adhering to the Mediterranean diet, this study emphasizes the critical role of interindividual variability in the complex polyphenols-gut ecosystem interrelationship at the microbiome level. According to the enterotype classification proposed by Arumugam et al. (2011), the bacterial microbiota of S1 (dominated by *Bifidobacterium*, *Phocaeicola*, and *Bacteroides*) corresponds to a Type-B enterotype (*Bacteroides*-dominated), while S2 (dominated by *Prevotella* and *Megamonas*) aligns with a Type-P enterotype (*Prevotella*-dominated). Although both SHIME® units were inoculated with fecal microbiota from donors adhering to a Mediterranean diet (well-documented to be associated with the *Bacteroidetes* phylum, including genera such as *Prevotella* and *Bacteroides* (De Filippis et al., 2016)), interindividual variability, potentially driven by host genetics, lifestyle and other intrinsic factors, resulted in distinct enterotype profiles (Zhernakova et al., 2024). This ecosystem variability reflects distinct microbiome changes in response to the supplementation with polyphenol-rich EBE, as different enterotypes harbor distinct commensal bacteria with specialized enzymes and different capacities to metabolize such compounds (Cantu-Jungles and Hamaker, 2020; Stevens et al., 2016). Interestingly, the sustained expansion of *Akkermansia muciniphila* observed in our *in vitro* model reflects the genus-level increase reported *in vivo* by Reider et al. (2022) using the same elderberry extract.

The F/B ratio is a useful biomarker of metabolic health: values above 2.0 have been linked to gut dysbiosis associated with type 2 diabetes, obesity, inflammatory diseases, COVID-19 complications (Petakh et al., 2023). The simulation showed that this ratio was modulated by EBE intake across all colon tracts, displaying distinct temporal patterns between SHIME® units. In particular, it lowered in both colon tracts of both SHIME® units to values that are below the baseline and the threshold value of 2.0, that is commonly associated with improved health outcomes (Koliada et al., 2017). Notably, the PC of S2, the only compartment with an initial F/B ratio above this limit (2.3 at baseline), exhibited a continuous decline during EBE intake, reaching 0.96 after the washout period, suggesting a potential beneficial impact of EBE in promoting the evolution to a more balanced gut microbiota profile.

Both the ecosystem-specific and the common shifts observed in bacterial community and pathway-associated genes following EBE intake suggest differential but converging potential beneficial effects across S1 and S2. Here, "individual-dependent" (ecosystem-specific) pathways refer to functional responses modulated in a donor-specific manner, reflecting baseline microbiota composition and metabolic capacity, whereas "individual-independent" (common-shift) pathways denote responses consistently modulated across SHIME® units irrespective of donor-specific microbial configurations. Overall, the more significant changes at T2 compared to T1 across all ecosystems hint at a delayed and time-dependent microbiome response to EBE intake. The presence of common trends on microbiota and functional pathway-associated gene changes highlighted some shared responses to EBE intake, like the temporal evolution of abundance of genes involved in the biosynthesis of various plant secondary metabolites and glycine,

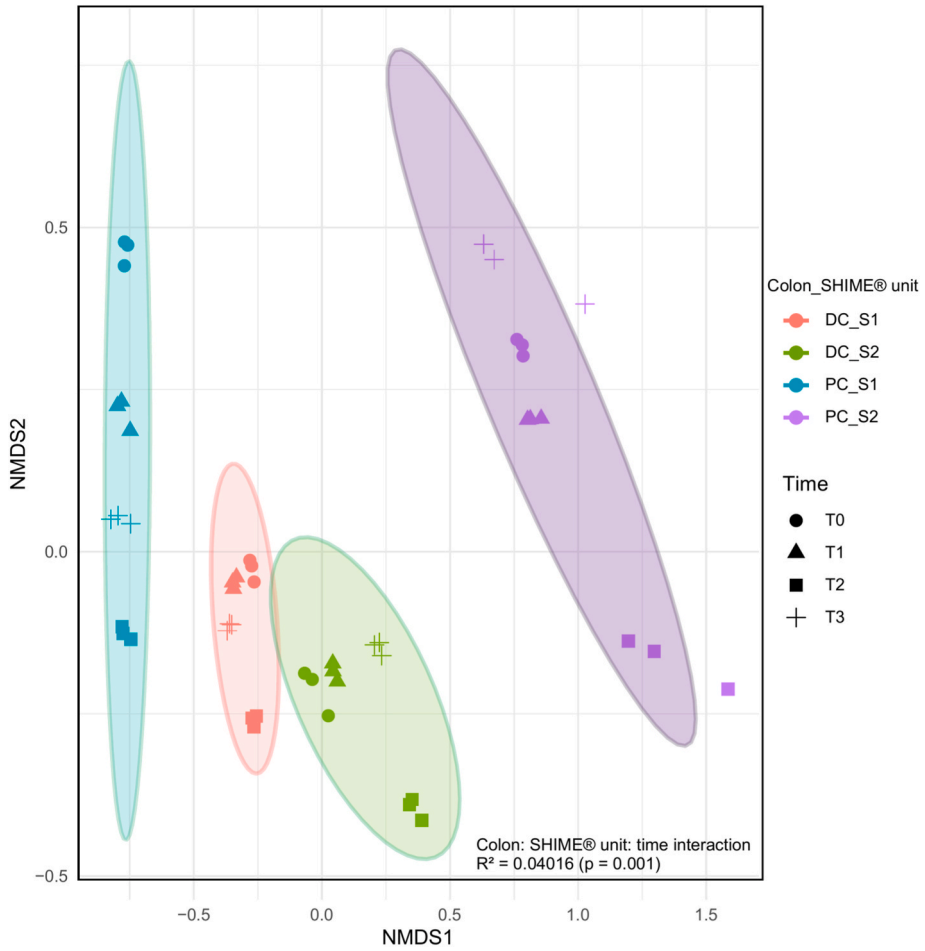

Fig. 4. Non-metric Multidimensional Scaling (NMDS) plot based on Jaccard's distance of functional profiles, comparing ecosystems after one (T1) and two (T2) weeks of elderberry extract intake, and after one week of washout (T3), relative to the baseline (T0), for both proximal colon (PC) and distal colon (DC) tracts of both SHIME® units (S1 and S2). Significant effects of SHIME® unit, colon tract, and time interaction were observed (all $P < 0.05$), assessed using PERMANOVA (Adonis2).

serine, and threonine metabolism in PCs of both S1 and S2, and those involved in glutathione metabolism in DCs of both S1 and S2. The glycine, serine, and threonine metabolism pathway is crucial for neurotransmitters production and gut barrier function through mucin production (Abdallah et al., 2020), and it was positively correlated with *P. diazotrophicus* in PC of S1, where the abundance of both pathway genes and species concurrently increased at T1 and T3. This finding is consistent with previous studies that highlighted the involvement of *Parabacteroides species* in amino acid metabolism, suggesting the contribution of *P. diazotrophicus* to the abundance of genes associated with such metabolism (Sakamoto & Benno, 2006). Similarly, the biosynthesis of various plant secondary metabolites, a pathway analogous to bacterial biosynthesis of phenolic derivatives such as urolithins, hydroxybenzoic acids, and gallic acid with potential anti-inflammatory and anti-cancer effects (Catalkaya et al., 2020), was positively associated with *C. butyricum*, *B. ovatus*, *P. distasonis*, and *B. longum* in the PC of S1. These species exhibited a concurrent abundance increase at T2 alongside genes involved in this pathway, suggesting their role in enhancing bioactive polyphenolic derivatives biosynthesis thanks to their enzymatic capacities in phenolic compounds metabolism (Braune, 2025; Kelly et al., 2018). In PCs of both SHIME® units, the increase in genes linked to the biosynthesis of various plant secondary metabolites at T2 corresponded with elevated TPC concentrations, with S1 showing relatively higher levels than S2. Glutathione metabolism plays a vital role in antioxidant defense, detoxification, and immune modulation (Hristov, 2022). In DCs, its concurrent increase at T2 with *E. coli*, *C. freundii*, *K. oxytoca*, *B. salyersiae*, and *P. diazotrophicus* in S1, and with *A. xylosoxidans* in S2 suggests a potential enhancement of antioxidative capacity due to EBE intake. Indeed, *C. freundii* and *K. oxytoca* are involved in maintaining oxidative stress resistance through the regeneration of glutathione and its role in neutralizing reactive oxygen species (Ibrahim et al., 2022), while *E. coli* is known to utilize glutathione for redox homeostasis and detoxification, and by consuming oxygen from the gut, it supports the establishment of a better habitat for other microorganisms (Smirnova et al., 2012). Differently, to the best of our knowledge, no relationships between *B. salyersiae*, *P. diazotrophicus*, or *A. xylosoxidans* and glutathione metabolism have been reported in literature. Such correlations most likely reflect indirect ecological associations rather than direct functional contributions.

Despite some common trends, several distinct and ecosystem-specific modulations emerged between S1 and S2. S1 was characterized by microbiome reshaping that can be linked to energy production, amino acid metabolism, and neuroactive compound synthesis. In PC, sphingolipid metabolism, neuroactive ligand-receptor interaction, and streptomycin biosynthesis genes were positively correlated with *P. dorei*, showing concurrent increases at T1. *P. dorei* is recognized as a microbial sphingolipid producer (Brown et al., 2019), and its expansion likely contributed to the observed increased abundance of genes associated with such metabolism. Sphingolipids are vital for nutrient absorption, gut barrier maintenance, and inflammatory regulation (Kim & Jazwinski, 2018; Li et al., 2024). Previous studies have linked *Parabacteroides species* to the production of neuroactive metabolites like gamma-aminobutyric acid (GABA) and indole derivatives (Otaru et al., 2021), which supports the observed positive correlation with genes

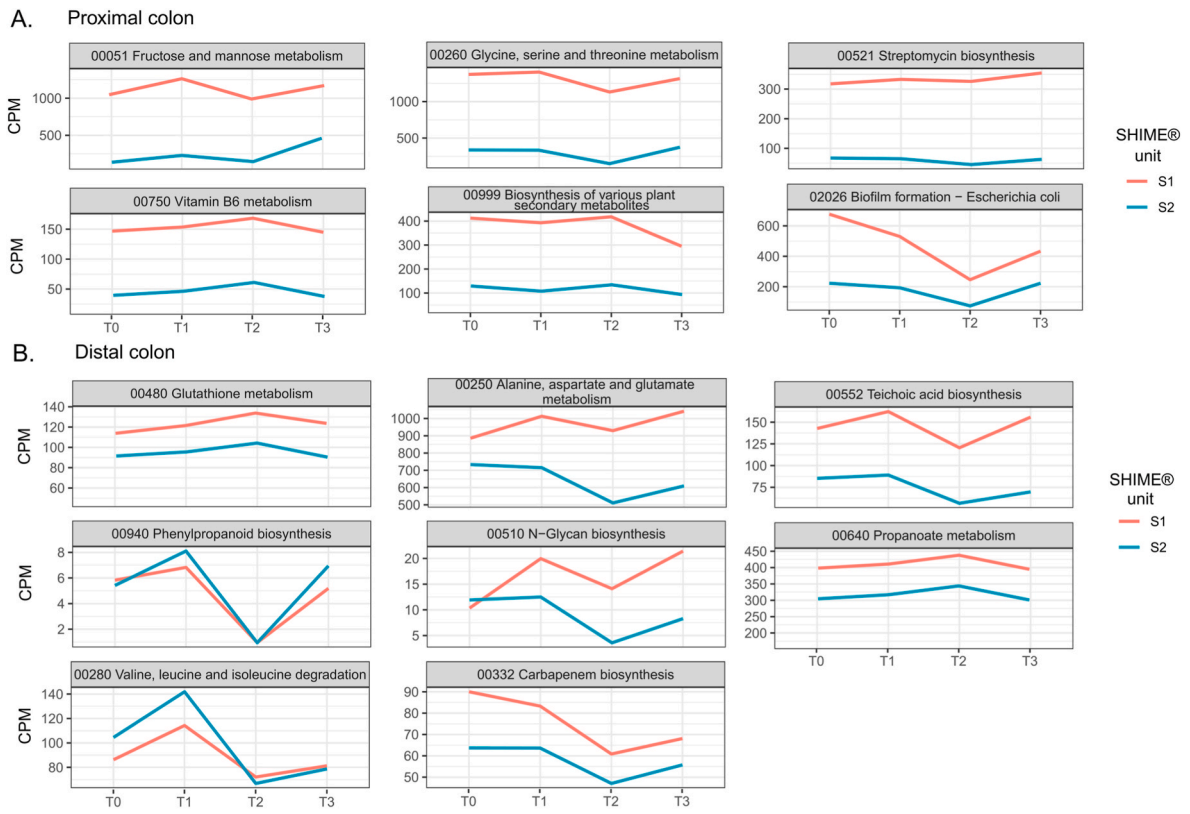

Fig. 5. Common trends in the abundance of functional pathway-associated genes across both SHIME® units (S1 and S2) in **(A)** the proximal colon (PC) and **(B)** the distal colon (DC) tracts at baseline (T0), after one (T1) and two (T2) weeks of elderberry extract intake, and after one week of washout (T3). Pathway-associated genes were included in the comparative analysis if they exhibited significant temporal changes in the PC or DC of at least one SHIME® unit, as determined by differential abundance analysis using MaAsLin2 with false discovery rate correction ($q < 0.05$; see Supplementary Fig. 4).

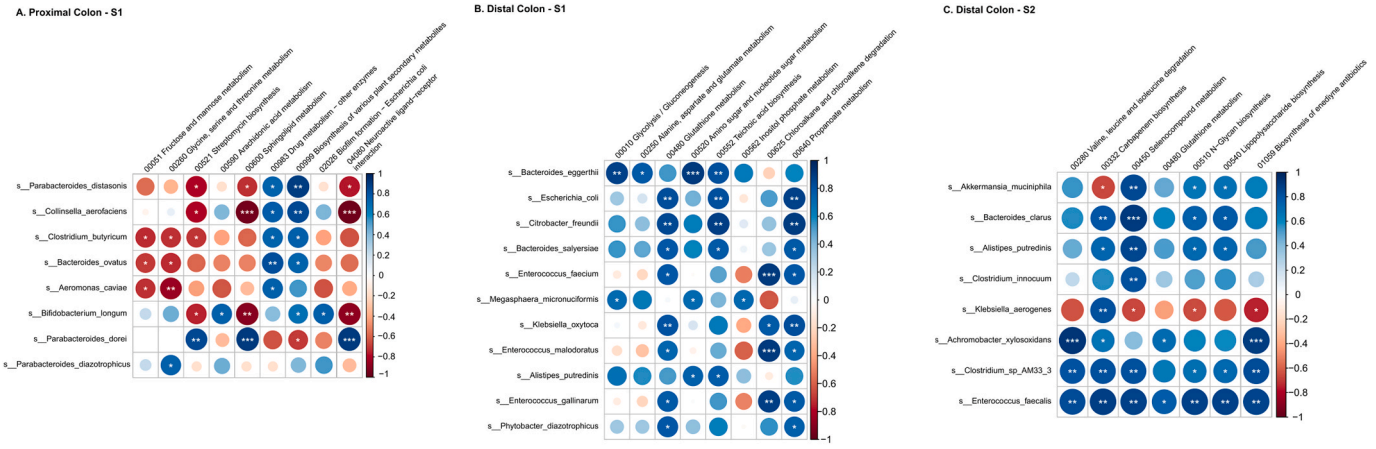

Fig. 6. Spearman correlations between differentially abundant bacterial species and Kyoto Encyclopedia of Genes and Genomes (KEGG) pathway-associated genes in **(A)** the proximal colon tract (PC) of SHIME® unit 1 (S1), **(B)** the distal colon tract (DC) of S1, and **(C)** the DC of SHIME® unit 2 (S2). False discovery rate (FDR) correction was applied to adjust for multiple comparisons. Species and pathway-associated genes were included in the analysis if they exhibited significant differential abundance in the PC or DC of at least one SHIME® unit. The PC of S2 was excluded from the analysis as no significant differential species abundance was detected. Asterisks indicate statistical significance of correlations: adjusted *P*-value (*padj*) < 0.05 (*), *padj* < 0.01 (**), and *padj* < 0.001 (***).

related to neuroactive ligand-receptor interactions and suggests potential beneficial effects on the microbiota-gut-brain axis. In DC, the positive correlation of glycolysis/gluconeogenesis and citrate cycle with *B. eggerthii*, which showed increased abundance at T2 and T3, highlights the potential contribution of this species to carbohydrate and fibers fermentation and energy generation, supporting gut microbiota's involvement in host metabolic processes (Ibrahim & Anishetty, 2012; Vernocchi et al., 2020). *B. eggerthii* also positively correlated with genes related to amino sugar and nucleotide sugar metabolism, which increased at T2 and T3. This is in agreement with the capacity of *Bacteroides species* to utilize complex glycans such as dietary fibers and host-derived glycosaminoglycans and glycoproteins, which release amino sugars like *N*-acetylglucosamine (Kmezik et al., 2021). These sugars are then metabolized via amino sugar and nucleotide sugar pathways to support cell wall biosynthesis and host-microbe interactions (Singh, 2019). Similarly, *A. putredinis* also positively

correlated with amino sugar and nucleotide sugar metabolism. However, its role in gut ecosystems is more controversial since it was associated with both beneficial (Wang et al., 2023) and detrimental effects (Watanabe et al., 2025) effects. Unfortunately, our analysis was not resolutive at the strain level, thus preventing a clear conclusion. Also, the positive correlation of the alanine, aspartate, and glutamate metabolism with *B. eggerthii*, showing increased abundance at T1 and T3, aligns with genomic evidence suggesting that *Bacteroides species*, including *B. eggerthii*, harbor genes supporting central amino acid metabolic pathways (Chen and Fang, 2025). At T2, the positive correlation between the increased abundance of genes involved in drug metabolism and *C. butyricum* is due to its capacity to metabolize polyphenols and participate in the biotransformation of xenobiotics, supporting its role in detoxification processes (Li et al., 2020; Pant et al., 2023). Genes linked to propanoate metabolism positively correlated with well-known SCFAs producers like *E. coli*, *C. freundii*, and *E. faecium* (Nakkarach et al., 2020; Zhu et al., 2024), which increased at T1. This finding explains the significant rise of acetic acid concentrations, a key precursor and intermediate in propanoate metabolism, observed in the same colon tract and time point.

Differently, the microbiome of S2 had shifts that potentially favored the biosynthesis of cell wall components, vitamins, and bioactive secondary metabolites, reflecting a distinct functional metabotype. In the PC of S2, changes in the abundances of several pathway-associated genes were observed, although they have not been associated with species dynamics according to Spearman correlation analysis. Specifically, the increases of genes linked to teichoic acid and arabinogalactan biosynthesis (at T1 and T3) and vitamin B6 metabolism (at T2 and T3) suggest relevant potential evolutions. In fact, teichoic acid and arabinogalactan biosynthesis contribute to bacterial cell wall reinforcement and enhanced resilience against environmental stressors, potentially influencing host immune modulation (Alderwick et al., 2015; Wu et al., 2020), while the vitamin B6 metabolism is essential for neurotransmitter synthesis, and its enhancement following polyphenol intake aligns with previous studies (Duda-Chodak et al., 2015). In the DC of S2, the positive correlation, at T1, of genes associated with valine, leucine, and isoleucine degradation and *A. xylosoxidans* can be attributed to the ability of such species for amino acid metabolism, including branched-chain amino acid catabolism, a process that is crucial for energy production and homeostatic balance (Zhang et al., 2023). The positive correlation of genes linked to selenocompound metabolism and *B. clarus*, *A. putredinis*, *C. innocuum*, *Clostridium* sp. AM33_3, and *E. faecalis*, which increased at T2, is coherent both with the capacity of *Bacteroides* and *Enterococcus species* to metabolize selenium, contributing to the gut's antioxidative capacity (Zhang et al., 2023), and the ability of *Alistipes* and *Clostridium species* to reduce selenite to selenide, which is essential for cellular function and resistance to oxidative stress (Wells & Stolz, 2020). At T2, the decrease in carbapenem biosynthesis genes was positively correlated with a reduction in *K. aerogenes* and negatively correlated with an increase in *A. muciniphila*. *K. aerogenes* degrades carbapenems to survive under competitive and inflammatory conditions (Takei et al., 2024). This ecological shift may have favored the proliferation of *A. muciniphila*, a beneficial microbe adapted to stable and low-competitive gut environments (Cani & de Vos, 2017; Zhai et al., 2019).

The overall higher propionic and acetic acid concentrations at baseline (T0) in S2 align with previous findings by De Filippis et al. (2016), who linked Type-P enterotypes, dominated by *Prevotella*, to elevated levels of these SCFAs. During the intervention, EBE intake led to an increase in acetic acid concentrations in the DC of both SHIME® units (at T1 in S1; at T2 in S2), demonstrating its capacity to enhance acetate production. Likewise, the observed rise in propionic acid in both colon tracts of S1 (at T1 and T2 in PC; at T2 in DC) reflects the microbiota evolution induced by EBE, which increased the abundance of SCFAs producers. SCFAs are well known to support gut barrier integrity, exert anti-inflammatory activity, and modulate immune responses (Yao et al., 2022). Nevertheless, literature on the impact of polyphenol intake (timing of treatment and daily dose) on SCFAs biosynthesis is non-univocal (Du et al., 2023; Zhang et al., 2022). The diversity of studied ecosystems and the different structures of used polyphenols, dietary fiber types, and dosages (all factors impacting SCFAs production at the gut level) can explain the controversy of the results (Zhang et al., 2025). Our study used a moderate daily dose (600 mg) of EBE, which corresponds to the polyphenol intake recommended by the WHO (Reider et al., 2022), providing 91.2 mg of anthocyanins but only 63.6 mg of dietary fiber. This amount of fiber is relatively low compared to the recommended daily intake of 25 g (WHO, 2023) and can explain the more contained SCFAs evolution. Despite the low daily dietary fiber supply, it has most probably acted as a co-substrate or carrier, facilitating microbial access to polyphenols and modulating their metabolic conversion into SCFAs (Bindels et al., 2015). In contrast, Wallace et al. (2015), who administered higher daily doses (750 mg polyphenols and 7.5 g fiber), reported no significant differences in SCFAs levels resulting from the intake of only polyphenols and fiber-polyphenol combinations, in either mouse or human fecal samples. However, the SHIME® model employed in our study offers a more physiologically relevant simulation of human gut ecology than static fecal incubations, and the fiber-driven SCFAs production is contingent on its structural properties and the host's microbial ecology (Vinelli et al., 2022). Moreover, the variability in SCFAs outcomes across both SHIME® units and colon tracts in our study reinforces the ecosystem-specific nature of microbiome responses, where individual microbial configurations influence the production and types of SCFAs (Tuohy et al., 2003).

Collectively, these findings suggest that the observed donor-dependent responses are driven by differences in baseline microbiota composition, functional gene repertoires, and metabolic capacity across distinct gut ecosystem configurations, consistent with enterotype-associated traits. However, although the adopted *in vitro* model represents the most suitable technology to obtain preliminary insights into gut ecosystem impacts, some aspects limiting the possibility to generalize the outcomes and to directly translate the findings to *in vivo* human outcomes should be considered. First, the SHIME® model, while enabling controlled and reproducible investigation of gut microbial processes, does not fully capture host-related factors such as immune interactions, epithelial responses, and systemic metabolism. Second, the use of one donor per enterotype (although accurately selected) limits the biological replicates and broad generalizability of conclusions. Finally, further studies including multiple nutritionally relevant doses and phenolic profiling in lumen samples following EBE supplementation will be necessary for a dose-response assessment and to provide a deeper insight into the fate of individual flavonoids, respectively.

5. Conclusion

Precision in nutrition requires designing supplementation strategies that consider inter-individual variability, which can improve the efficacy of dietary interventions. Such *in vitro* simulation through the SHIME® model opened a perspective on the potential evolution of different gut ecosystems after the intake of the elderberry extract rich in polyphenols and fiber. Despite the inter-individual features being the main drivers differentiating the gut ecosystems, the intake of elderberry extract resulted in significant, and mainly donor-dependent, modulations of microbiome with several potentially beneficial effects. Although this *in vitro* approach represents a simplification compared to the conditions to which gut microbiota are subjected *in vivo*, and *in vivo* studies will be necessary to better reveal the spectrum of effects induced by the extract intake, the findings opened the window into the different and promising ecological evolutions induced by EBE intake in different gut ecosystems, suggesting its suitability for personalized diets. Personalization may involve adapting EBE supplementation duration or dose according to microbiome responsiveness, enterotype-associated traits, and functional capacity for polyphenol and SCFAs metabolism.

However, *in vivo* validation combined with targeted metabolomic profiling will be required before translating these insights into actionable dietary recommendations.

CRediT authorship contribution statement

Francis Aheto: Writing – review & editing, Writing – original draft, Visualization, Methodology, Investigation, Formal analysis, Data curation. **Lena Granehäll:** Visualization, Software, Formal analysis, Data curation. **Olga Nikoloudaki:** Writing – review & editing, Visualization, Validation, Formal analysis, Data curation. **Martina Ben:** Methodology, Formal analysis. **Stephan Plattner:** Writing – review & editing, Project administration. **Marco Gobbetti:** Writing – review & editing, Project administration, Funding acquisition. **Raffaella Di Cagno:** Writing – review & editing, Project administration, Funding acquisition. **Andrea Polo:** Writing – review & editing, Supervision, Project administration, Funding acquisition, Data curation, Conceptualization.

Ethics approval and consent to participate

The collection of data from consumers and the use of human fecal samples were conducted in accordance with the Declaration of Helsinki and approved by the Ethics Committee of the Free University of Bozen on July 17, 2019.

Funding sources

The APC was funded by the Open Access Publishing Fund of the Free University of Bozen-Bolzano.

Declaration of competing interest

The authors declare that they have no known competing financial interests or personal relationships that could have appeared to influence the work reported in this paper.

Acknowledgments

The authors thank Dr. Sara Casagrande Bacchiocchi, Dr. Federica Mastrolonardo and Dr. Stefano Tonini for their help throughout this research.

Appendix A. Supplementary data

Supplementary data to this article can be found online at https://doi.org/10.1016/j.fbio.2026.108442.

Data availability

Sequence data and metadata for the samples in this study are deposited at the National Center for Biotechnology Information (NCBI) Sequence Read Archive (SRA) under the BioProject number PRJNA1293117 (https://www.ncbi.nlm.nih.gov/bioproject/PRJNA1293117).

References

Abdallah, A., Elemba, E., Zhong, Q., & Sun, Z. (2020). Gastrointestinal interaction between dietary amino acids and gut microbiota: With special emphasis on host nutrition. *Current Protein & Peptide Science, 21*(8), 785–798. https://doi.org/10.2174/1389203721666200212095503

Arumugam, M., Raes, J., Pelletier, E., Le Paslier, D., Yamada, T., Mende, D. R., Fernandes, G. R., Tap, J., Bruls, T., Batto, J.-M., Bertalan, M., Borruel, N., Casellas, F., Fernandez, L., Gautier, L., Hansen, T., Hattori, M., Hayashi, T., Kleerebezem, M., … Bork, P. (2011). Enterotypes of the human gut microbiome. *Nature, 473*(7346), 174–180. https://doi.org/10.1038/nature09944

Bäckhed, F., Fraser, C. M., Ringel, Y., Sanders, M. E., Sartor, R. B., Sherman, P. M., Versalovic, J., Young, V., & Finlay, B. B. (2012). Defining a healthy human gut microbiome: Current concepts, future directions, and clinical applications. *Cell Host & Microbe, 12*(5), 611–622. https://doi.org/10.1016/j.chom.2012.10.012

Beghini, F., McIver, L. J., Blanco-Míguez, A., Dubois, L., Asnicar, F., Maharjan, S., Mailyan, A., Manghi, P., Scholz, M., Thomas, A. M., Valles-Colomer, M., Weingart, G., Zhang, Y., Zolfo, M., Huttenhower, C., Franzosa, E. A., & Segata, N. (2021). Integrating taxonomic, functional, and strain-level profiling of diverse microbial communities with bioBakery 3. *eLife, 10*, Article e65088. https://doi.org/10.7554/eLife.65088

Beresford-Jones, B. S., Forster, S. C., Stares, M. D., Notley, G., Viciani, E., Browne, H. P., Boehmler, D. J., Soderholm, A. T., Kumar, N., Vervier, K., Cross, J. R., Almeida, A., Lawley, T. D., & Pedicord, V. A. (2022). The mouse gastrointestinal bacteria catalogue enables translation between the mouse and human gut microbiotas via functional mapping. *Cell Host & Microbe, 30*(1), 124–138.e8. https://doi.org/10.1016/j.chom.2021.12.003

Bindels, L. B., Delzenne, N. M., Cani, P. D., & Walter, J. (2015). Towards a more comprehensive concept for prebiotics. *Nature Reviews Gastroenterology & Hepatology, 12*(5), 303–310. https://doi.org/10.1038/nrgastro.2015.47

Blanco-Míguez, A., Beghini, F., Cumbo, F., McIver, L. J., Thompson, K. N., Zolfo, M., Manghi, P., Dubois, L., Huang, K. D., Thomas, A. M., Nickols, W. A., Piccinno, G., Piperni, E., Punčochář, M., Valles-Colomer, M., Tett, A., Giordano, F., Davies, R., Wolf, J., … Segata, N. (2023). Extending and improving metagenomic taxonomic profiling with uncharacterized species using MetaPhlAn 4. *Nature Biotechnology, 41*(11), 1633–1644. https://doi.org/10.1038/s41587-023-01688-w

Braune, A. (2025). Flavonoid-converting capabilities of *Clostridium butyricum*. *Applied Microbiology and Biotechnology, 109*(1), 53. https://doi.org/10.1007/s00253-025-13434-0

Bresciani, L., Angelino, D., Vivas, E. I., Kerby, R. L., García-Viguera, C., Del Rio, D., Rey, F. E., & Mena, P. (2020). Differential catabolism of an anthocyanin-rich elderberry extract by three gut microbiota bacterial species. *Journal of Agricultural and Food Chemistry, 68*(7), 1837–1843. https://doi.org/10.1021/acs.jafc.9b00247

Brown, E. M., Ke, X., Hitchcock, D., Jeanfavre, S., Avila-Pacheco, J., Nakata, T., Arthur, T. D., Fornelos, N., Heim, C., Franzosa, E. A., Watson, N., Huttenhower, C., Haiser, H. J., Dillow, G., Graham, D. B., Finlay, B. B., Kostic, A. D., Porter, J. A., Vlamakis, H., … Xavier, R. J. (2019). Bacteroides-derived sphingolipids are critical for maintaining intestinal homeostasis and symbiosis. *Cell Host & Microbe, 25*(5), 668–680.e7. https://doi.org/10.1016/j.chom.2019.04.002

Cantu-Jungles, T. M., & Hamaker, B. R. (2020). New view on dietary fiber selection for predictable shifts in gut microbiota. *mBio, 11*(1). https://doi.org/10.1128/mBio.02179-19

Catalkaya, G., Venema, K., Lucini, L., Rocchetti, G., Delmas, D., Daglia, M., De Filippis, A., Xiao, H., Quiles, J. L., Xiao, J., & Capanoglu, E. (2020). Interaction of dietary polyphenols and gut microbiota: Microbial metabolism of polyphenols, influence on the gut microbiota, and implications on host health. *Food Frontiers, 1*(2), 109–133. https://doi.org/10.1002/fft2.25

Centers for Disease Control and Prevention (CDC). (2022). *State indicator report on fruits and vegetables, 2022. Division of nutrition, physical activity, and obesity*. National Center for Chronic Disease Prevention and Health Promotion. Retrieved from https://www.cdc.gov/nutrition/data-statistics/2022-state-indicator-report-fruits-vegetables.html. (Accessed 10 April 2024).

Chen, Y., & Fang, J.-Y. (2025). The role of colonic microbiota amino acid metabolism in gut health regulation. *Cell Insight, 4*(2), Article 100227. https://doi.org/10.1016/j.cellin.2025.100227

Chen, S., Zhou, Y., Chen, Y., & Gu, J. (2018). Fastp: An ultra-fast all-in-one FASTQ preprocessor. *Bioinformatics, 34*(17), i884–i890. https://doi.org/10.1093/bioinformatics/bty560

Da Ros, A., Polo, A., Rizzello, C. G., Acin-Albiac, M., Montemurro, M., Di Cagno, R., & Gobbetti, M. (2021). Feeding with sustainably sourdough bread has the potential to promote the healthy microbiota metabolism at the Colon level. *Microbiology Spectrum, 9*(3). https://doi.org/10.1128/Spectrum.00494-21

De Filippis, F., Pellegrini, N., Vannini, L., Jeffery, I. B., La Storia, A., Laghi, L., Serrazanetti, D. I., Di Cagno, R., Ferrocino, I., Lazzi, C., Turroni, S., Cocolin, L., Brigidi, P., Neviani, E., Gobbetti, M., O'Toole, P. W., & Ercolini, D. (2016). High-level adherence to a Mediterranean diet beneficially impacts the gut microbiota and associated metabolome. *Gut, 65*(11), 1812–1821. https://doi.org/10.1136/gutjnl-2015-309957

De Paepe, K., Verspreet, J., Courtin, C. M., & Van de Wiele, T. (2020). Microbial succession during wheat bran fermentation and colonisation by human faecal microbiota as a result of niche diversification. *The ISME Journal, 14*(2), 584–596. https://doi.org/10.1038/s41396-019-0550-5

Du, L., Lü, H., Chen, Y., Yu, X., Jian, T., Zhao, H., Wu, W., Ding, X., Chen, J., & Li, W. (2023). Blueberry and blackberry anthocyanins ameliorate metabolic syndrome by modulating gut microbiota and short-chain fatty acids metabolism in high-fat diet-fed C57BL/6J mice. *Journal of Agricultural and Food Chemistry, 71*(40), 14649–14665. https://doi.org/10.1021/acs.jafc.3c04606

Duda-Chodak, A., Tarko, T., Satora, P., & Sroka, P. (2015). Interaction of dietary compounds, especially polyphenols, with the intestinal microbiota: A review. *European Journal of Nutrition, 54*(3), 325–341. https://doi.org/10.1007/s00394-015-0852-y

Eurostat. (2022). *Fruit and vegetable consumption statistics in the EU, 2022*. Statistical Office of the European Union. https://doi.org/10.2908/HLTH_EHIS_FV3E. . (Accessed 10 April 2024)

Graf, D., Di Cagno, R., Fåk, F., Flint, H. J., Nyman, M., Saarela, M., & Watzl, B. (2015). Contribution of diet to the composition of the human gut microbiota. *Microbial Ecology in Health and Disease, 26*(0). https://doi.org/10.3402/mehd.v26.26164

Gutiérrez-Díaz, I., Fernández-Navarro, T., Sánchez, B., Margolles, A., & González, S. (2016). Mediterranean diet and faecal microbiota: A transversal study. *Food & Function, 7*(5), 2347–2356. https://doi.org/10.1039/C6FO00105J

Hristov, B. D. (2022). The role of glutathione metabolism in chronic illness development and its potential use as a novel therapeutic target. *Cureus, 14*(9). https://doi.org/10.7759/cureus.29696

Ibrahim, M., & Anishetty, S. (2012). A meta-metabolome network of carbohydrate metabolism: Interactions between gut microbiota and host. *Biochemical and Biophysical Research Communications, 428*(2), 278–284. https://doi.org/10.1016/j.bbrc.2012.10.045

Ibrahim, M. S., Çakmak, M., Özer, D., Karataş, F., & Saydam, S. (2022). Effect of cadmium and vitamin C on *citrobacter freundii*'s antioxidant enzymes and stress markers. *Afyon Kocatepe University Journal of Sciences and Engineering, 22*(1), 23–32. https://doi.org/10.35414/akufemubid.1007756

Kelly, S. M., O'Callaghan, J., Kinsella, M., & van Sinderen, D. (2018). Characterisation of a hydroxycinnamic acid esterase from the *Bifidobacterium longum* subsp. longum taxon. *Frontiers in Microbiology, 9*. https://doi.org/10.3389/fmicb.2018.02690

Kerimi, A., Kraut, N. U., da Encarnacao, J. A., & Williamson, G. (2020). The gut microbiome drives inter- and intra-individual differences in metabolism of bioactive small molecules. *Scientific Reports, 10*(1), Article 19590. https://doi.org/10.1038/s41598-020-76558-5

Kim, S., & Jazwinski, S. M. (2018). The gut microbiota and healthy aging: A mini-review. *Gerontology, 64*(6), 513–520. https://doi.org/10.1159/000490615

Kmezik, C., Krska, D., Mazurkewich, S., & Larsbrink, J. (2021). Characterization of a novel multidomain CE15-GH8 enzyme encoded by a polysaccharide utilization locus in the human gut bacterium *Bacteroides eggerthii*. *Scientific Reports, 11*(1), Article 17662. https://doi.org/10.1038/s41598-021-96659-z

Koliada, A., Syzenko, G., Moseiko, V., Budovska, L., Puchkov, K., Perederiy, V., Gavalko, Y., Dorofeyev, A., Romanenko, M., Tkach, S., Sineok, L., Lushchak, O., & Vaiserman, A. (2017). Association between body mass index and firmicutes/bacteroidetes ratio in an adult Ukrainian population. *BMC Microbiology, 17*(1), 120. https://doi.org/10.1186/s12866-017-1027-1

Li, L.-L., Amara, R., Souissi, S., Dehaut, A., Duflos, G., & Monchy, S. (2020). Impacts of microplastics exposure on mussel (*Mytilus edulis*) gut microbiota. *Science of The Total Environment, 745*, Article 141018. https://doi.org/10.1016/j.scitotenv.2020.141018

Li, H., Liang, J., Han, M., & Gao, Z. (2024). Polyphenols synergistic drugs to ameliorate non-alcoholic fatty liver disease via signal pathway and gut microbiota: A review. *Journal of Advanced Research*. https://doi.org/10.1016/j.jare.2024.03.004

Manning, T. S., & Gibson, G. R. (2004). Prebiotics. *Best Practice & Research Clinical Gastroenterology, 18*(2), 287–298. https://doi.org/10.1016/j.bpg.2003.10.008

Martinez, K. B., Leone, V., & Chang, E. B. (2017). Western diets, gut dysbiosis, and metabolic diseases: Are they linked? *Gut Microbes, 8*(2), 130–142. https://doi.org/10.1080/19490976.2016.1270811

Młynarczyk, K., Walkowiak-Tomczak, D., & Łysiak, G. P. (2018). Bioactive properties of *Sambucus nigra* L. as a functional ingredient for food and pharmaceutical industry. *Journal of Functional Foods, 40*, 377–390. https://doi.org/10.1016/j.jff.2017.11.025

Molly, K., Vande Woestyne, M., & Verstraete, W. (1993). Development of a 5-step multi-chamber reactor as a simulation of the human intestinal microbial ecosystem. *Applied Microbiology and Biotechnology, 39*(2), 254–258. https://doi.org/10.1007/BF00228615

Nabizadeh, E., Sadeghi, J., Rezaee, M. A., Hamishehkar, H., Hasani, A., Kafil, H. S., Sharifi, Y., Asnaashari, S., Kadkhoda, H., & Ghotaslou, R. (2023). The profile of key gut microbiota members and short-chain fatty acids in patients with sepsis. *Heliyon, 9*(7), Article e17880. https://doi.org/10.1016/j.heliyon.2023.e17880

Nakkarach, A., Foo, H. L., Song, A. A.-L., Nitisinprasert, S., & Withayagiat, U. (2020). Promising discovery of beneficial *Escherichia coli* in the human gut. *3 Biotech, 10*(7), 296. https://doi.org/10.1007/s13205-020-02289-z

Otaru, N., Ye, K., Mujezinovic, D., Berchtold, L., Constancias, F., Cornejo, F. A., Krzystek, A., de Wouters, T., Braegger, C., Lacroix, C., & Pugin, B. (2021). GABA production by human intestinal *bacteroides* spp.: Prevalence, regulation, and role in acid stress tolerance. *Frontiers in Microbiology, 12*. https://doi.org/10.3389/fmicb.2021.656895

Pandey, K. R., Naik, S. R., & Vakil, B. V. (2015). Probiotics, prebiotics and synbiotics - A review. *Journal of Food Science and Technology, 52*(12), 7577–7587. https://doi.org/10.1007/s13197-015-1921-1

Pant, A., Maiti, T. K., Mahajan, D., & Das, B. (2023). Human gut microbiota and drug metabolism. *Microbial Ecology, 86*(1), 97–111. https://doi.org/10.1007/s00248-022-02081-x

Petakh, P., Oksenych, V., & Kamyshnyi, A. (2023). The F/B ratio as a biomarker for inflammation in COVID-19 and T2D: Impact of metformin. *Biomedicine & Pharmacotherapy, 163*, Article 114892. https://doi.org/10.1016/j.biopha.2023.114892

Plamada, D., & Vodnar, D. C. (2021). Polyphenols-gut microbiota interrelationship: A transition to a new generation of prebiotics. *Nutrients, 14*(1), 137. https://doi.org/10.3390/nu14010137

Polo, A., Albiac, M. A., Da Ros, A., Ardèvol, V. N., Nikoloudaki, O., Verté, F., Di Cagno, R., & Gobbetti, M. (2023). The effect of hydrolyzed and fermented arabinoxylan-oligo saccharides (AXOS) intake on the middle-term gut microbiome modulation and its metabolic answer. *Nutrients, 15*(3), 590. https://doi.org/10.3390/nu15030590

Reider, S., Watschinger, C., Längle, J., Pachmann, U., Przysiecki, N., Pfister, A., Zollner, A., Tilg, H., Plattner, S., & Moschen, A. R. (2022). Short- and long-term effects of a prebiotic intervention with polyphenols extracted from european black elderberry—sustained expansion of *Akkermansia* spp. *Journal of Personalized Medicine, 12*(9), 1479. https://doi.org/10.3390/jpm12091479

Rodríguez-Daza, M. C., Pulido-Mateos, E. C., Lupien-Meilleur, J., Guyonnet, D., Desjardins, Y., & Roy, D. (2021). Polyphenol-mediated gut microbiota modulation: Toward prebiotics and further. *Frontiers in Nutrition, 8*. https://doi.org/10.3389/fnut.2021.689456

Sakamoto, M., & Benno, Y. (2006). Reclassification of *Bacteroides distasonis, Bacteroides goldsteinii* and *Bacteroides merdae* as *Parabacteroides distasonis* gen. nov., comb. nov., *Parabacteroides goldsteinii* comb. nov. and *Parabacteroides merdae* comb. nov. *International Journal of Systematic and Evolutionary Microbiology, 56*(7), 1599–1605. https://doi.org/10.1099/ijs.0.64192-0

Severino, A., Tohumcu, E., Tamai, L., Dargenio, P., Porcari, S., Rondinella, D., Venturini, I., Maida, M., Gasbarrini, A., Cammarota, G., & Ianiro, G. (2024). The microbiome-driven impact of western diet in the development of noncommunicable chronic disorders. *Best Practice & Research Clinical Gastroenterology, 72*, Article 101923. https://doi.org/10.1016/j.bpg.2024.101923

Shen, W., Sipos, B., & Zhao, L. (2024). SeqKit2: A Swiss Army knife for sequence and alignment processing. *iMeta, 3*(3), Article e191. https://doi.org/10.1002/imt2.191

Singh, R. P. (2019). Glycan utilisation system in *bacteroides* and *Bifidobacteria* and their roles in gut stability and health. *Applied Microbiology and Biotechnology, 103*(18), 7287–7315. https://doi.org/10.1007/s00253-019-10012-z

Singleton, V. L., & Rossi, J. A. (1965). Colorimetry of total phenolics with phosphomolybdic-phosphotungstic acid reagents. *American Journal of Enology and Viticulture, 16*(3), 144–158. https://doi.org/10.5344/ajev.1965.16.3.144

Smirnova, G., Muzyka, N., & Oktyabrsky, O. (2012). Transmembrane glutathione cycling in growing *Escherichia coli* cells. *Microbiological Research, 167*(3), 166–172. https://doi.org/10.1016/j.micres.2011.05.005

Stevens, J. F., & Maier, C. S. (2016). The chemistry of gut microbial metabolism of polyphenols. *Phytochemistry Reviews, 15*(3), 425–444. https://doi.org/10.1007/s11101-016-9459-z

Teets, C., Ghanem, N., Ma, G., Minj, J., Perkins-Veazie, P., Johnson, S. A., Etter, A. J., Carbonero, F. G., & Solverson, P. M. (2024). A one-week elderberry juice intervention augments the fecal microbiota and suggests improvement in glucose tolerance and fat oxidation in a randomized controlled trial. *Nutrients, 16*(20), 3555. https://doi.org/10.3390/nu16203555

Tlais, A. Z. A., Da Ros, A., Filannino, P., Vincentini, O., Gobbetti, M., & Di Cagno, R. (2021). Biotechnological re-cycling of apple by-products: A reservoir model to produce a dietary supplement fortified with biogenic phenolic compounds. *Food Chemistry, 336*, Article 127616. https://doi.org/10.1016/j.foodchem.2020.127616

Tuohy, K. M., Probert, H. M., Smejkal, C. W., & Gibson, G. R. (2003). Using probiotics and prebiotics to improve gut health. *Drug Discovery Today, 8*(15), 692–700. https://doi.org/10.1016/S1359-6446(03)02746-6

Van den Abbeele, P., Grootaert, C., Marzorati, M., Possemiers, S., Verstraete, W., Gérard, P., Rabot, S., Bruneau, A., El Aidy, S., Derrien, M., Zoetendal, E., Kleerebezem, M., Smidt, H., & Van de Wiele, T. (2010). Microbial community development in a dynamic gut model is reproducible, colon region specific, and selective for *Bacteroidetes* and *Clostridium* Cluster IX. *Applied and Environmental Microbiology, 76*(15), 5237–5246. https://doi.org/10.1128/AEM.00759-10

Vernocchi, P., Del Chierico, F., & Putignani, L. (2020). Gut microbiota metabolism and interaction with food components. *International Journal of Molecular Sciences, 21*(10), 3688. https://doi.org/10.3390/ijms21103688

Vinelli, V., Biscotti, P., Martini, D., Del Bo', C., Marino, M., Meroño, T., Nikoloudaki, O., Calabrese, F. M., Turroni, S., Taverniti, V., Unión Caballero, A., Andrés-Lacueva, C., Porrini, M., Gobbetti, M., De Angelis, M., Brigidi, P., Pinart, M., Nimptsch, K., Guglielmetti, S., & Riso, P. (2022). Effects of dietary fibers on short-chain fatty acids and gut microbiota composition in healthy adults: A systematic review. *Nutrients, 14*(13), 2559. https://doi.org/10.3390/nu14132559

Wallace, A. J., Eady, S. L., Hunter, D. C., Skinner, M. A., Huffman, L., Ansell, J., Blatchford, P., Wohlers, M., Herath, T. D., Hedderley, D., Rosendale, D., Stoklosinski, H., McGhie, T., Sun-Waterhouse, D., & Redman, C. (2015). No difference in fecal levels of bacteria or short chain fatty acids in humans, when consuming fruit juice beverages containing fruit fiber, fruit polyphenols, and their combination. *Nutrition Research, 35*(1), 23–34. https://doi.org/10.1016/j.nutres.2014.11.002

Wang, Q., Huang, H., Yang, Y., Yang, X., Li, X., Zhong, W., Wen, B., He, F., & Li, J. (2024). Reinventing gut health: Leveraging dietary bioactive compounds for the prevention and treatment of diseases. *Frontiers in Nutrition, 11*. https://doi.org/10.3389/fnut.2024.1491821

Wang, K., Mehta, R. S., Ma, W., Nguyen, L. H., Wang, D. D., Ghazi, A. R., Yan, Y., Al-Shaar, L., Wang, Y., Hang, D., Fu, B. C., Ogino, S., Rimm, E. B., Hu, F. B., Carmody, R. N., Garrett, W. S., Sun, Q., Chan, A. T., Huttenhower, C., & Song, M. (2023). The gut microbiome modifies the associations of short- and long-term physical activity with body weight changes. *Microbiome, 11*(1), 121. https://doi.org/10.1186/s40168-023-01542-w

Watanabe, N., Watari, T., Hosokawa, N., & Otsuka, Y. (2025). Alistipes bacteremia in older patients with digestive and cancer comorbidities, Japan, 2016–2023. *Emerging Infectious Diseases, 31*(4). https://doi.org/10.3201/eid3104.241284

Wells, M., & Stolz, J. F. (2020). Microbial selenium metabolism: A brief history, biogeochemistry and ecophysiology. *FEMS Microbiology Ecology, 96*(12). https://doi.org/10.1093/femsec/fiaa209

World Health Organization. (2023). Increasing fruit and vegetable consumption to reduce the risk of noncommunicable diseases. Retrieved from https://www.who.int/tools/elena/interventions/fruit-vegetables-ncds. (Accessed 10 April 2024).

Wu, Y., Han, Y., Tao, Y., Li, D., Xie, G., Show, P. L., & Lee, S. Y. (2020). In vitro gastrointestinal digestion and fecal fermentation reveal the effect of different encapsulation materials on the release, degradation and modulation of gut microbiota of blueberry anthocyanin extract. *Food Research International, 132*, Article 109098. https://doi.org/10.1016/j.foodres.2020.109098

Xiao, J. (2022). Recent advances on the stability of dietary polyphenols. *eFood, 3*(3). https://doi.org/10.1002/efd2.21

Yang, L., Hung, L. Y., Zhu, Y., Ding, S., Margolis, K. G., & Leong, K. W. (2022). Material engineering in gut microbiome and human health. *Research: Ideas for Today's Investors, 2022*, Article 9804014. https://doi.org/10.34133/2022/9804014

Yao, Y., Cai, X., Fei, W., Ye, Y., Zhao, M., & Zheng, C. (2022). The role of short-chain fatty acids in immunity, inflammation and metabolism. *Critical Reviews in Food Science and Nutrition, 62*(1), 1–12. https://doi.org/10.1080/10408398.2020.1854675

Zhai, Q., Feng, S., Arjan, N., & Chen, W. (2019). A next generation probiotic, *Akkermansia muciniphila*. *Critical Reviews in Food Science and Nutrition, 59*(19), 3227–3236. https://doi.org/10.1080/10408398.2018.1517725

Zhang, Y., Chang, H., Shao, S., Zhao, L., Zhang, R., & Zhang, S. (2022). Anthocyanins from *Opuntia ficus-indica* modulate gut microbiota composition and improve short-chain fatty acid production. *Biology, 11*(10), 1505. https://doi.org/10.3390/biology11101505

Zhang, S., Niu, H., & Zhu, J. (2025). Personalized nutrition studies of human gut microbiome-polyphenol interactions utilizing continuous multistaged in vitro fermentation models–a narrative review. *Nutrition Research, 135*, 101–127. https://doi.org/10.1016/j.nutres.2025.01.011

Zhang, H., Wang, Z., Wang, G., Song, X., Qian, Y., Liao, Z., Sui, L., Ai, L., & Xia, Y. (2023). Understanding the connection between gut homeostasis and psychological stress. *The Journal of Nutrition, 153*(4), 924–939. https://doi.org/10.1016/j.tjnut.2023.01.026

Zhernakova, D. V., Wang, D., Liu, L., Andreu-Sánchez, S., Zhang, Y., Ruiz-Moreno, A. J., Peng, H., Plomp, N., Del Castillo-Izquierdo, Á., Gacesa, R., Lopera-Maya, E. A., Temba, G. S., Kullaya, V. I., van Leeuwen, S. S., Aguirre-Gamboa, R., Deelen, P., Franke, L., Kuivenhoven, J. A., Nolte, I. M., … Fu, J. (2024). Host genetic regulation of human gut microbial structural variation. *Nature, 625*(7996), 813–821. https://doi.org/10.1038/s41586-023-06893-w

Zhu, Y., Yin, C., & Wang, Y. (2024). Probiotic *Enterococcus faecium* attenuated atherosclerosis by improving SCFAs associated with gut microbiota in ApoE−/− mice. *Bioengineering, 11*(10), 1033. https://doi.org/10.3390/bioengineering11101033